Simulation and Sensitivity Analysis of Cold Wave Event Impact on Transmission Grid Infrastructure

Brent Austgen, Alejandro D. Owen Aquino
Electric Power Systems Research Dept.
Sandia National Laboratories
Albuquerque, NM, USA
{bgaustg,adowena}@sandia.gov

Adam B. Birchfield, Joshua Xia, Thomas J. Overbye
Dept. of Electrical and Computer Engineering
Texas A&M University
College Station, TX, USA
{abirchfield,joshua_x,overbye}@tamu.edu

Austen Barker, Thomas M. Kroeger
Cyber Ops. Research and Engineering Dept.
Sandia National Laboratories
Livermore, CA, USA
{atbarke,tmkroeg}@sandia.gov

***Abstract*— We present an integrated framework to simulate cold wave impacts on bulk power systems by combining a temperature-conditioned stochastic generator outage model with 5-minute time-sequential power-flow simulations and an operator-inspired load-shedding controller. The approach is demonstrated on the Texas2k synthetic grid using Winter Storm Uri data and compared against a 1949 cold wave scenario to quantify sensitivity of reserves and load shed to weather-driven outages.**

I. Introduction

Winter Storm Uri brought record low temperatures to many parts of Texas and surrounding states in February 2021, causing extensive generator outages and resulting in an energy crisis on the Texas electric interconnect, requiring operators to shed up to 20 GW of load over the course of three days, narrowly avoiding an uncontrolled system blackout [1]. This event highlighted the complex interactions between weather, interdependent infrastructure, electric grid performance and operator decisions over the course of a multi-day scenario. It underscored the importance of modeling and simulation capabilities for evaluating how temporally and spatially varying environmental and technical parameters affect overall system performance.

Prior to Uri, several studies have looked at various aspects of infrastructure impacts of cold weather and related events. For example, in [2], the authors apply a probabilistic risk framework focused on distribution lines that employs a Monte Carlo-type evaluation method to estimate customer outage likelihood. In [3] and [4] the authors focus on transmission lines under various types of extreme weather, using fragility curves and resilience metrics based on a formulated optimization problem. Since Uri, the attention has increasingly shifted to generation resource availability, with studies such as [5] looking at energy portfolio optimization, and [6] proposing a methodology to pick the right investments to decrease the risk of another energy crisis. Even more recently, authors in [7] employ a machine learning technique, trained on extensive outage data, to predict weather-induced component outages and resulting energy disruptions.

For many parts of Texas, Feb. 2021 was *not* the lowest temperature on record, with records set before the emergence of today's expansive electric transmission network. In some places, the coldest weather on record was winter of 1899 or 1949 [8]. The existence of historical data in the context of grid impact assessment and sensitivity gives the opportunity to examine how different historical events, if they were to occur in today's grid, could potentially affect electric service availability.

This paper makes two main contributions. First, it presents an integrated framework for simulation and sensitivity analysis of cold-weather events on electric grid infrastructure. Second, it applies this framework in sensitivity case studies to demonstrate the impact of the February 2021 and January/February 1949 events on the Texas2k Series 25 synthetic transmission model of Texas [9]-[10] with 2021 scale transmission and generation capacity. In the remainder of this paper, we present our contributions in Section II, an application of those contributions in Section III, and our conclusions in Section IV.

II. Cold-Weather Impacts Integrated Framework

The following section presents a new framework for simulating the impact of cold-weather events on the electric power grid. The framework combines a stochastic generator outage model based on historical Winter Storm Uri data with time-sequential power grid simulations and an operator-driven load-shedding decision model.

A. Stochastic Generator Outage Model

We propose a temperature-conditioned stochastic thermal generator outage model designed to be parametrized using historical generator outage/derate data and surface temperature data aligned on uniform time periods. Our model is notionally similar to that from [6], which we extend to include a temporal dimension. For each generator g and time period t we compute a normalized generator availability ratio

$$A_{gt} = \frac{C_g - \Delta C_{gt}}{C_g} \in [0,1],$$

where C_g is the generator's capacity and $\Delta C_{gt} \in [0, C_g]$ is its capacity loss at time period t. Let $\mathcal{F}$ denote the set of generator fuel types, and let $\mathcal{G}_f$ be the set of generators of fuel type $f \in \mathcal{F}$. We discretize availability using thresholds specific to generator fuel types. The threshold is defined to be the smallest $\tau \in [0,1]$ such that capacity loss (MWh) for the discretized outages does not exceed that for the reference outages/derates:

$$\tau_f^* = \inf_{\tau \in [0,1]} \left\{ d \sum_{g \in \mathcal{G}_f} \sum_{T_{gt} \in b} 1_{[A_{gt} < 1-\tau]} C_{gt} \leq d \sum_{g \in \mathcal{G}_f} \sum_{T_{gt} \in b} \Delta C_{gt} \right\}.$$

This work was supported by the U.S. Department of Energy, National Nuclear Security Administration, and performed at Sandia National Laboratories, a multimission laboratory managed and operated by National Technology and Engineering Solutions of Sandia, LLC, for DOE/NNSA under contract DE-NA0003525.

Copyright ©2026 IEEE. Personal use of this material is permitted. IEEE International Conference on Communications, Control, and Computing Technologies for Smart Grids (SmartGridComm) 2026, College Station, TX, October 2026.

Above, d represents the time period duration. For each fuel type f, we compute τ_f^* via bisection.

To estimate temperature-conditioned failure probabilities, we establish indicators for two types of events in the discretized outage data: an uptime indicator U_{gt} that is 1 only if generator g is not affected by an outage at time period t and a downtime start indicator D_{gt}^{start} that is 1 only if generator g suffers an outage event starting at time period t. Subsequent outage periods are excluded from analysis (i.e., we suppose a generator cannot fail when already in a failed state). We let T_{gt} denote the surface temperature of generator g at time period t. For a temperature bin b (defined by its lower/upper edges) and fuel type f, we estimate the generator failure probability as the empirical outage-start rate:

$$p_f(b) = \frac{\sum_{g\in\mathcal{G}_f}\sum_{t:T_{gt}\in b} D_{gt}^{\text{start}}}{\sum_{g\in\mathcal{G}_f}\sum_{t:T_{gt}\in b}\left(U_{gt} + D_{gt}^{\text{start}}\right)},$$

which may be used to sample generator outage events. To determine the duration of an outage, we propose fitting and sampling from distributions using the durations of the discretized outage events.

B. Simulation Architecture and Methodology

Power grid simulations within the proposed cold-weather integrated framework are based on quasi-steady-state power flow (PF) models of electric transmission systems. For this analysis, we use PowerWorld Simulator [11] with input and output functions provided by the Easy SimAuto package [12]. PF simulations are generally considered valid for time steps of five minutes or longer, so this span was chosen as the granularity of the time series framework. Though further fidelity could be achieved with dynamic or transient simulations, the key outage and response aspects of electric grid operation during cold-weather events can be represented with sequential PF.

Running sequential PF simulations requires an initial snapshot of the grid's state, followed by variations at each time interval. Therefore, the architecture can be divided into two parts: (1) pre-simulation procedures that initialize PFs at each time step and incorporate state changes carried over from the previous step, and (2) post-solution procedures which measure and record important output and trigger control actions.

Within the proposed architecture, system load demand is drawn from historical data and generally considered to be fixed. While future efforts could incorporate load-forecasting methods to capture load variations due to external factors such as weather, this is outside the scope of the present study. Historical data must consider real-life outages and load-shedding events for the inputs to the simulations to reflect true load demand rather than merely load served. Then, during simulation, the modeled loads are reduced according to any corresponding triggered load-shed events as we explain in Section II.C.

Generation data are the most complex inputs to each PF time step. For solar and wind units, known time of day and geographically tagged weather data can be used to specify the generator availability. Alternatively, historical data can be used if wind and solar historical outputs are known. Generation outages, which are at the core of cold-weather simulations, can be determined either based on a historical or probabilistic (see Section II.A) approach. Once the generator outages, renewable availability, and load demands are known, generator dispatch is performed based on a generation control scheme, which could be economic or participation-factor-based. In doing so, there is also a need to consider ramping constraints.

Once the load, generation, and other input data are passed to the network solver and the solution is retrieved, the post-processing steps compile the key output variables for analysis and determine the control actions (e.g. operator-triggered load shedding) to be implemented in future time steps.

C. Operator Load Shedding Model

Power system operators intentionally shed load if spinning reserves are inadequate for satisfying anticipated future demand. Generally, an operator will enter emergency operation conditions, exhausting other less severe control options before initiating an intentional load reduction [13].

Modeling load shedding in full fidelity is complex because it requires representing human operational response and decision-making. For the purposes of this framework, we apply the relatively simple load shedding procedure outlined in Algorithm 1, where $G_{\text{t,}}^{\max} L_{\text{t}}^{\text{d}}, L_{\text{t}}^{\text{f}}, L_{\text{t}}^{\text{shed}}$, and P_{t}^{r} represent the total available generation, total load demand, load scaling factor, load shed, and spinning reserves at time t, respectively.

The exact thresholds for Algorithm 1 may be adjusted for specific situations, but the framework is generally designed to capture the main characteristics of a typical load shedding scheme. If not already shedding ($L_{\text{t}}^{\text{shed}} = 0$), then the algorithm does not shed unless reserves are very low, and then it does so aggressively to ensure grid stability. Once in load shedding conditions, the controller targets a pre-specified reserve level, which should be around the largest potential generator outage event (4000-6000 MW in the Texas2k case). If reserves are sufficient, it slowly restores load, up to 500 MW per half hour.

Algorithm 1: Load Shed/Restoration Controller (Δt = 5min)

Require: At each time *t* (after each PF)*:* $(G_{\text{t,}}^{\max}, L_{\text{t}}^{\text{d}}, L_{\text{t}}^{\text{f}}, L_{\text{t}}^{\text{shed}})$

1: $P_{\text{t}}^{\text{r}} \leftarrow G_{\text{t,}}^{\max} - L_{\text{t}}^{\text{d}} \times L_{\text{t}}^{\text{f}}$

2: **if** $P_{\text{t}}^{\text{r}} < 800$ **then**

Order ← 3500 MW

elseif ($P_{\text{t}}^{\text{r}} < 4000$) **and** ($L_{\text{t}}^{\text{shed}} > 0$) **and** ($L_{\text{t}}^{\text{shed}} = L_{\text{t}-6}^{\text{shed}}$) **then**

Order ← 1500 MW

elseif ($P_{\text{t}}^{\text{r}} > 6000$) **and** ($L_{\text{t}}^{\text{shed}} > 0$) **and** ($L_{\text{t}}^{\text{shed}} = L_{\text{t}-6}^{\text{shed}}$) **then**

Order ← -500 MW

3: $L_{\text{t+1}}^{\text{shed}} \leftarrow max\left(0, L_{\text{t}}^{\text{shed}} + \text{Order}\right)$

4: $L_{\text{t+1}}^{\text{f}} \leftarrow \frac{L_{\text{t}}^{\text{d}} \times L_{\text{t}}^{\text{f}} + L_{\text{t}-1}^{\text{shed}} - L_{\text{t}}^{\text{shed}}}{L_{\text{t}}^{\text{d}} \times L_{\text{t}}^{\text{f}} + L_{\text{t}-1}^{\text{shed}}}$

III. Case Studies for 2021 and 1949 Winter Storms

Using the framework discussed in the previous section we have simulated stochastic outage scenarios based on 2021's Winter Storm Uri and the Winter Storm of late January 1949.

A. Historical Benchmark for 2021 Winter Storm Uri

To provide an initial benchmark, we emulate Winter Storm Uri by running simulations driven by historical storm-period data. This subsection describes the curation of load, wind, solar, and generator outage datasets to match the historical data onto the Texas2k synthetic grid.

1) Load Profile

Publicly available ERCOT data from 2021 contains hourly actual loads for eight weather zones [14], along with system-wide estimated load shed [15]. Several steps for processing this input data for this study are taken. First, the load data given as hourly values are linearly interpolated to 5-minute time series. Second, the load shed data is split into the areas, proportional to the area's actual load at each time instance. Third, the area-wide loads are split into bus-level loads in the Texas2k synthetic case, proportional to the bus's peak load in the base synthetic case. Resulting load data is shown in Figure 1.

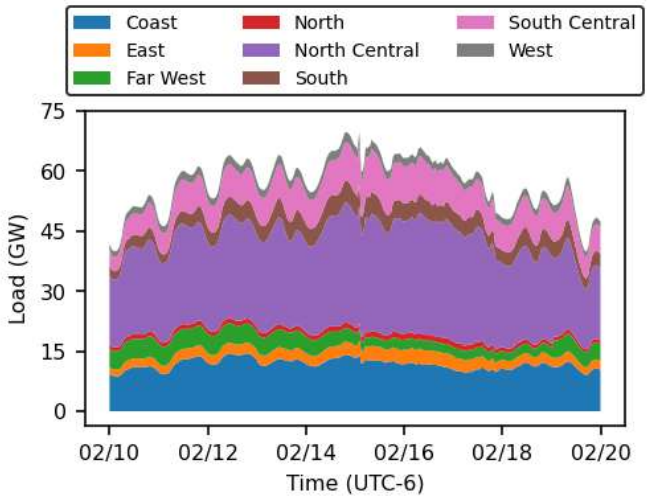

Figure 1: Time series of system-wide load (partitioned by weather zones) used in the simulations.

2) Wind and Solar Profile

Similar to the load profile, we want a Texas2k-based wind and solar profile to match the wind and solar outputs during Uri. We start with the historical wind and solar hourly ERCOT Uri data [16], [17]. and perform another five-minute interpolation, similar to what was done for the load profile. Figure 2 shows the system-wide aggregate profiles used in the study.

3) Generator Outages

The last piece of historical data we need are generator outages. Publicly available outage information for Uri contains the longitudes and latitudes (which match exactly to those in the synthetic case), outage duration, fuel types, and generator capacity derates for all generators [18]. Figure 3 shows time series for the total number of synchronous generator outages and power derates during the storm.

Although the available datasets provide detailed information on the generator outages, the corresponding generator definitions do not exactly match those in the Texas2k synthentic case. In the historical records, multiple generators at the same substation are often represented as separate units with distinct IDs, a situation commonly observed with wind generation. By contrast, the Texas2k case aggregates these units, making it appear as though only a single generator exists at the substation. As a result, when several units (at the same substation) experience outages at the same time in the historical data, derating a single aggregated generator in the Texas2k case does not always cleanly approximate the real outages. In some cases, the combined historical outages would require a derate larger than what the aggregated Texas2k generator can support. This results in our model having less outaged capacity than what actually occurred. Additionally, some of the historical generators' locations, fuel types, and MW capacities do not match with any of those in the Texas2k case.

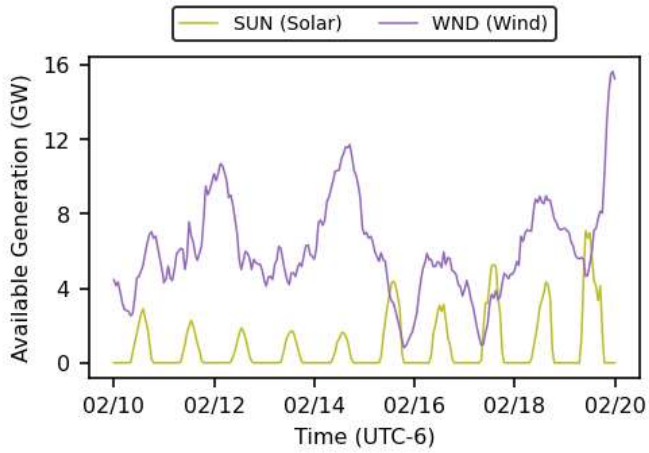

Figure 2: Time series of available solar and wind generation.

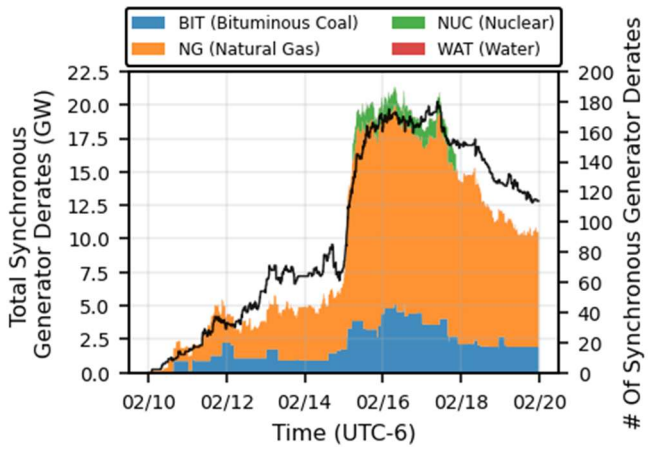

Figure 3: Time series of synchronous generator derated capacity by fuel type (left axis) and outage/derate event count (right axis).

To address these inconsistencies between data sets we map each historical outage to a unique generator in the Texas2k case.

For each historical outage we assemble a list of top 20 closest Texas2k generators, sorted first by closest location followed by closest MW capacity. Outages are binned into corresponding 5-minute intervals. For each outage during each interval, we iterate through the outage's list of candidate Texas2k generators, and pair it with the first yet unmatched generator in the list. This way, even if the locations don't exactly match or the Texas2k generator MW capacity would have been exceeded, each historical outage gets a mapping to a unique generator in the synthetic case.

B. *Cold-Weather Impacts Integrated Framework Results on 2021 Winter Storm Uri*

We used 5-minute resolution ERCOT outage/derate data [18] and gridded MERRA-2 reanalysis temperature data [19] from Feb. 10-19, 2021 (UTC-6) to parametrize a stochastic generator outage model using the methodology in Section II.A. For the duration of bituminous coal (BIT) and natural gas (NG) generator outages, we fit and sampled from truncated normal distributions based on the average, standard deviation, minimum, and maximum of the discretized historical outage data. These statistics are shown in Table 1. For the duration of nuclear (NUC) and hydroelectric (WAT) generator outages, we assign degenerate distributions based on a lone observation of event duration for each type.

Table 1: Outage Duration (5-Minute Periods) Statistics by Fuel Type

Fuel Type	μ (avg.)	σ (std. dev.)	a (min.)	b (max.)
BIT	432.29	594.31	26	2272
NG	396.93	526.77	1	2754
NUC	764	N/A	764	764
WAT	1407	N/A	1407	1407

Using the parametrized outage model, we sampled 100 outage scenarios to represent the uncertainty in cold-weather generator performance. Across the 100 simulations, we held all parameters constant other than the generator outages. We used these outage scenarios to assess the impact of an uncertain cold-weather event using the simulation methodology from Sections II.B and II.C.

Figure 4 shows multiple quantiles of generation capacity loss, generation reserves, and load shed as time series compared to those in the base case historical simulations. The top subplot also highlights the probability of exceeding 5, 10, 15 and 20 GW of generation capacity loss at any given time across scenarios. The system suffered capacity loss in excess of 15 GW for some period of time in all simulations. Capacity loss in excess of 20 GW was only suffered in 38% of the simulations. An interesting aspect of the temperature-driven stochastic outage model is that its outage samples sometimes induce simulated load shed noticeably earlier or later than in the base case. For example, we observe that many simulations featured load shed on Feb. 12-14 and Feb. 19. Meanwhile, for the key period of Feb. 15-18 the median load shed across scenarios closely approximates the shape and magnitude of the load shed in the base historical simulation.

In Figure 5, we highlight the relationship between overall generation capacity loss by fuel type and overall load shed across all simulated scenarios. For each fuel type, the Pearson correlation coefficient for generation capacity loss of that fuel type with load shed is given in the corresponding scatter plot. Observe that among these fuel types, load shed is most strongly correlated with NG generator outages, followed closely by BIT. In contrast, NUC and WAT outages are weakly correlated with load shed. Natural gas and coal generators are abundant in the Texas2k case, and they are also quite susceptible to failure according to the parametrized stochastic outage model's failure probabilities. It is intuitive that load shed is strongly correlated with capacity loss for generators with those fuel types.

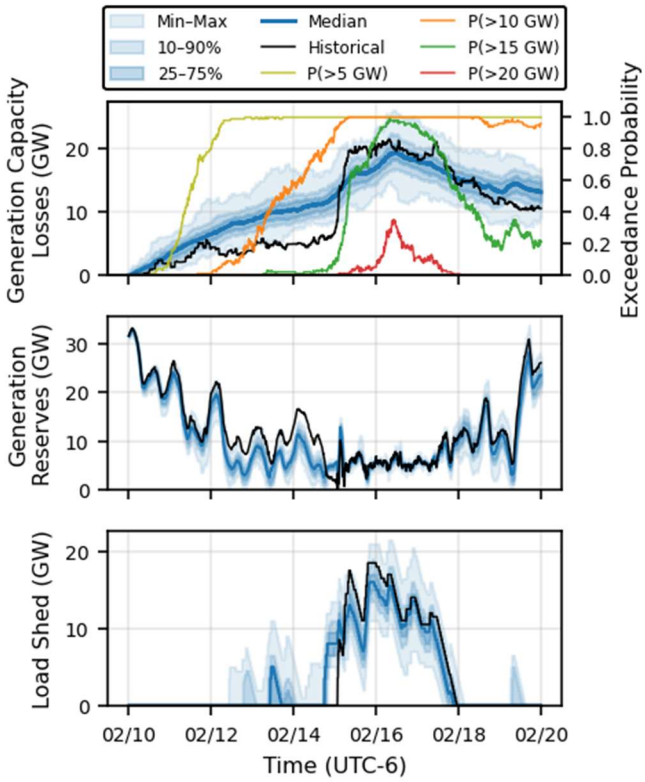

Figure 4: Time series for quantiles of generation capacity losses, generation reserves, and load shed across the 100 sampled 2021 outage scenarios.

Data from the base historical case are drawn as black points in Figure 5, and that data all lie near the borders of the simulated data. The primary reason for this is that the base historical case features both outages and derates, but the sampled cases, which are obtained through a process that discretizes the historical derates, feature only outages. That is, the methodology we propose has the potential to introduce bias in the samples. For the data we present, bias is most evident in the loss of natural gas generator capacity. Also, the Texas2k case features four nuclear generators of similar capacity; consequently, capacity-loss realizations for this fuel type lie in one of five bands, each

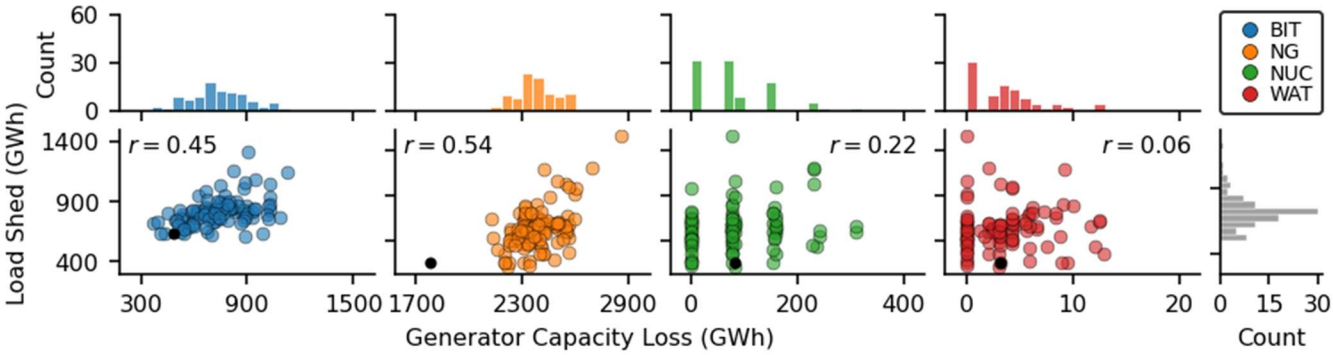

Figure 5: Relationships between overall generation capacity loss for each fuel type and overall load shed in the 2021 event simulations. Scatter plot points are semi-transparent so that regions dense with points are more apparent. The base historical case is rep

band corresponding to a number of generator outages between zero and four.

C. Sensitivity Analysis and Comparison to 1949 Winter Storm

To further test and demonstrate our methodology, we sample 100 additional outage scenarios using ERA5 temperature data [20] from the 1949 winter storm and simulate their impact. For these simulations, we shift the temperature data from January 25-February 4, 1949, to February 10-19, 2021. The 1949 cold temperatures are comparable in duration and severity to Uri, and this shift aligns the temperature troughs of the two events so that we may use the former event's temperature time series with the temporal inputs we prepared to simulate Uri (i.e., load, and solar, and wind). For the 1949 simulations, Figure 6 shows multiple quantiles of generation capacity loss, generation reserves, and load shed as time series.

Figure 4 and Figure 6 have striking similarities, which highlights that the sampled 2021 and 1949 outage scenarios, respectively, have a comparable simulated impact on the Texas2k case. Much of the similarity, especially that in the generation reserves, may be attributed to the simulations' shared load and wind/solar generation time series. The notable difference in impact is that the 1949 event's peak load shed tends to be slightly worse than that for the 2021 event; however, load shed in the days before and after the height of the storm is less severe. With respect to overall load shed, a comparison of the right-most histograms in Figure 5 and Figure 7 shows that the simulated 2021 outages are slightly more impactful.

Interestingly, across all generator fuel types with forced outages, overall generator capacity loss is more strongly correlated with overall load shed in the 1949 simulations than in the 2021 simulations. Though investigation is beyond the scope of this paper, plausible reasons for this include different spatial coincidence of temperature with certain generator types, different spatial coincidence of outages and load, and outages forcing generation reserves toward or away from the load shed controller thresholds for longer periods of time.

IV. Conclusions

This paper presented an integrated framework for assessing cold wave impacts on bulk power systems that couples a temperature-conditioned stochastic generator outage model with 5-minute time-sequential power-flow simulations and an operator-inspired load-shedding and restoration controller. Applied to the Texas2k synthetic grid and parameterized using Winter Storm Uri outage and temperature data, the Monte Carlo results reproduced key features of the event, including the timing and magnitude of reserve depletion and load shedding, while also illustrating how discretizing derates into outages can shift historical outcomes toward the boundary of the simulated distributions.

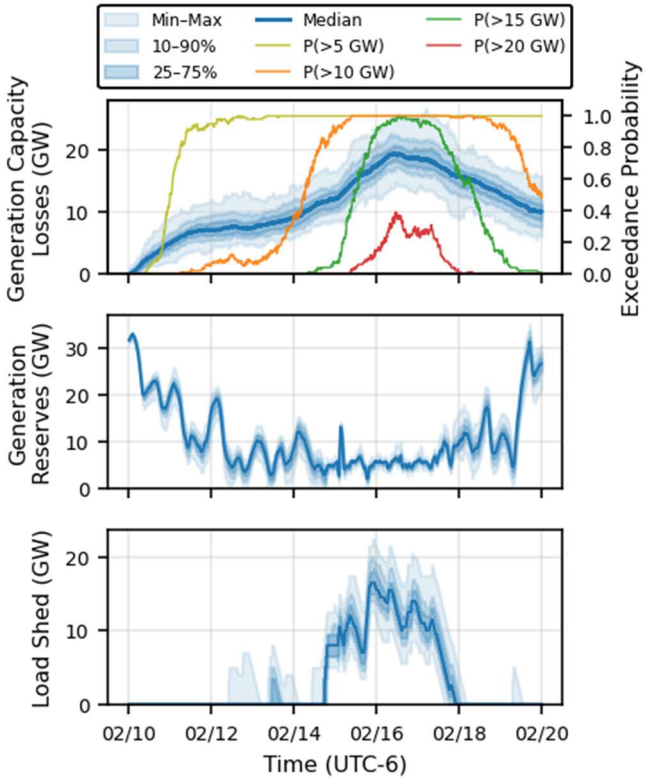

Figure 6: Time series for quantiles of generation capacity losses, generation reserves, and load shed across the 100 sampled 1949 outage scenarios (shifted in time to align with Uri's dates).

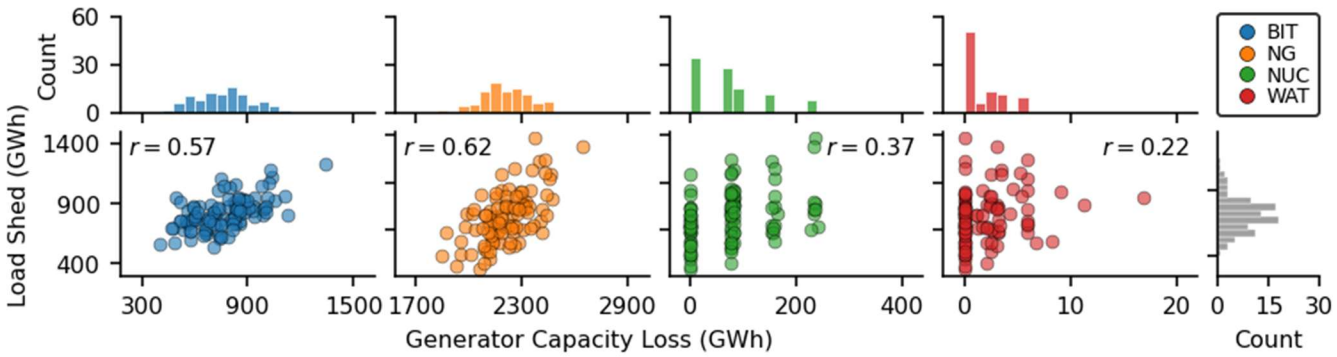

Figure 7: Relationships between overall generation capacity loss for each fuel type and overall load shed in the 1949 event simulations. Scatter plot points are semi-transparent so that regions dense with points are more apparent.

We also demonstrated the framework's use for sensitivity analysis by simulating 100 additional scenarios driven by temperature conditions from the 1949 cold wave (time-shifted to align with the Uri input profiles). The 1949-based simulations produced impacts comparable to the Uri-based simulations, with modest differences in peak versus shoulder-period load shedding, indicating that multiple historical cold extremes could plausibly stress today's system to similar degrees. Future work will focus on reducing discretization bias (e.g., explicitly modeling derates) and incorporating explicit natural gas infrastructure modeling to better represent fuel-supply constraints and correlated gas-generator performance during cold-weather events.

REFERENCES

[1] *The February 2021 Cold Weather Outages in Texas and the South Central United States.* Federal Energy Regulatory Commission (FERC), North American Electric Reliability Corporation (NERC), and Regional Entity Staff Report, Nov. 2021. Online: https://www.nerc.com/globalassets/our-work/reports/event-reports/february_2021_cold_weather_report.pdf

[2] G. Li et al., "Risk Analysis for Distribution Systems in the Northeast U.S. Under Wind Storms," *IEEE Trans. Power Syst.*, vol. 29, no. 2, pp. 889-898, Mar. 2014.

[3] M. Panteli, C. Pickering, S. Wilkinson, R. Dawson and P. Mancarella, "Power System Resilience to Extreme Weather: Fragility Modeling, Probabilistic Impact Assessment, and Adaptation Measures," *IEEE Trans. Power Syst.*, vol. 32, no. 5, pp. 3747-3757, Sep. 2017.

[4] M. Panteli and P. Mancarella, "Modeling and Evaluating the Resilience of Critical Electrical Power Infrastructure to Extreme Weather Events," *IEEE Syst. J.*, vol. 11, no. 3, pp. 1733-1742, Sept. 2017.

[5] A. Chaidez and Y. Sang, "Optimal Energy Portfolio Planning for Power System Considering the Impact of Winter Storms," *2021 North American Power Symposium (NAPS)*, College Station, TX, USA, 2021, pp. 1-5.

[6] B. G. Austgen et al., "Three-Stage Optimization Model to Inform Risk-Averse Investment in Power System Resilience to Winter Storms," *IEEE Access*, vol. 12, pp. 135117-135134, 2024.

[7] J. Lee, S. Lee, S. Chinthavali and S. Paal, "A Near-Real-Time Model for Predicting Electricity Disruptions in Texas During Winter Storms," *IEEE Access*, vol. 13, pp. 139583-139603, 2025.

[8] R. A. Bolinger et al, "An assessment of the extremes and impacts of the February 2021 South-Central U.S. Arctic outbreak, and how climate services can help," *Weather Clim. Extremes*, vol. 36, Jun. 2022.

[9] A.B. Birchfield, T. Xu, K.M. Gegner, K.S. Shetye, and T.J. Overbye, "Grid Structural Characteristics as Validation Criteria for Synthetic Networks," *IEEE Trans. Power Syst*, vol. 32, no. 4, pp. 3258-3265, Jul. 2017.

[10] J. Baek and A. B. Birchfield, "A tuning method for exciters and governors in realistic synthetic grids with dynamics," 2023 North American Power Symposium (NAPS), Asheville, NC, USA, Oct. 2023, pp. 1-6.

[11] *PowerWorld Simulator*. PowerWorld Corporation. Apr. 2026. Online: https://www.powerworld.com/products/simulator/overview

[12] B.L. Thayer, Z. Mao, Y. Liu, K. Davis and T. Overbye, "Easy SimAuto (ESA): A Python Package that Simplifies Interacting with PowerWorld Simulator," *J. Open Source Software*, vol. 5, no. 50, pp. 2289, Jun. 2020.

[13] *Ercot's use of Energy Emergency Alerts*. Energy Reliability Council of Texas (ERCOT). Sept 2020. Online: https://www.ercot.com/files/docs/2021/03/03/EEA_OnePager_updated_9-4-20.pdf

[14] *Actual System Load by Weather Zone.* Electric Reliability Council of Texas (ERCOT). Online: https://data.ercot.com/data-product-archive/NP6-345-CD

[15] *Available Generation and Estimated Load without Load Shed Data*. Electric Reliability Council of Texas (ERCOT). Apr. 2021. Online: https://www.ercot.com/files/docs/2021/03/18/Available_Generation_and_Estimated_Load_without_Load_Shed_Data.xlsx

[16] *Wind Power Production – Hourly Averaged Actual and Forecasted Values.* Electric Reliability Council of Texas (ERCOT). Online: https://www.ercot.com/mp/data-products/data-product-details?id=NP4-732-CD

[17] *Solar Power Production – Hourly Averaged Actual and Forecasted Values*. Electric Reliability Council of Texas (ERCOT). Online: https://www.ercot.com/mp/data-products/data-product-details?id=NP4-737-CD

[18] *ERCOT Winter Storm Generator Outages by Cause Updated Report.* Electric Reliability Council of Texas (ERCOT). Apr. 2021. Online: https://www.ercot.com/news/february2021

[19] *MERRA-2 const_2d_asm_Nx: 2d, constants V5.12.4.* Global Modeling and Assimilation Office (GMAO), Goddard Earth Sciences Data and Information Services Center (GES DISC). (accessed Apr 23 2026).

[20] H. Hersbach et al., "The ERA5 Global Reanalysis", in *Q. J. R. Meteorolog. Soc.*, vol. 146, no. 730, pp. 1999-2049, July 2020.